Network nonlocality sharing in a two-forked tree-shaped network

Hao Sun,[1,2,3] Fenzhuo Guo,[1,2,3,*] Haifeng Dong,[4] and Fei Gao[3]

[1]*School of Science, Beijing University of Posts and Telecommunications, Beijing 100876, China*
[2]*Henan Key Laboratory of Network Cryptography Technology, Zhengzhou 450001, China*
[3]*State Key Laboratory of Networking and Switching Technology, Beijing University of Posts and Telecommunications, Beijing 100876, China*
[4]*School of Instrumentation Science and Opto-Electronics Engineering, Beihang University, Beijing 100191, China*

(Received 20 December 2023; accepted 24 May 2024; published 1 July 2024)

Quantum network nonlocality sharing provides a unique perspective for constructing large-scale quantum networks and holds promise for numerous potential applications. In this paper we demonstrate the network nonlocality sharing via unsharp measurements in a two-forked n-layer tree-shaped network, which features $2^n - 2$ independent sources and $2^n - 1$ nodes. We investigate the $(2^n - 2)$-local scenarios via any m-sided sequential measurements, and conclude that arbitrarily many independent observers on each sequential side can share the non-$(2^n - 2)$-locality for a sufficiently large value of n. For a finite n, we present a method that enables directly obtaining the number of observers on each sequential side, who can share the non-$(2^n - 2)$-locality simultaneously. To interpret our results more intuitively, we discuss the simplest case of $n = 3$, and find that at most 30, 6, 3, and 2 sequential observers per sequential side can simultaneously share the non-6-locality in m-sided cases for $m = 1, 2, 3, 4$, respectively.

DOI: 10.1103/PhysRevA.110.012401

I. INTRODUCTION

A seminal concept distinguishing quantum mechanics from classical mechanics is Bell nonlocality. Bell's well-known theorem [1] provides us with experimentally testable criteria suitable for verifying Bell nonlocality by violating a Bell inequality. Specifically, when two separated observers perform local measurements on a pair of entangled particles distributed by a single source, correlations between measurement outcomes are said to be nonlocal, provided that they violate a Bell inequality. A series of Bell experiments [2–5] have been conducted to detect Bell nonlocality, including multipartite cases where all the separated parties receive their particles from a common source. Bell nonlocality has become a significant resource in a variety of quantum tasks, such as randomness expansion [6,7] and quantum key distribution [8].

With the development of quantum technology, long-distance and large-scale multiuser quantum networks become an important goal of quantum communication. Different from typical multipartite Bell experiments, the network Bell experiments contain more than one source. Quantum network nonlocality, a new form of multipartite nonlocality that may transcend typical Bell nonlocality, is fundamental for the quantum communication network. Quantum network nonlocality has been verified through the violation of suitable network Bell inequalities in various quantum networks [9–19], including the simplest bilocal networks [9,10], n-local chain-shaped networks [11], n-local star-shaped networks [12–15], and tree-shaped networks [16,17]. The network nonlocality has been used in device-independent frameworks, such as quantum key distribution [20], self-testing [21], and blind quantum computation [22].

Early works of the exploration of Bell nonlocality focused on the scenario where each particle from an entangled pair was measured once in a round of experiments. In 2015 Silva *et al.* [23] began to study whether many independent observers can sequentially measure one of the particles from an entangled system and share Bell nonlocality with a single observer on the other side. Since then, much attention has been devoted to detecting the sharing of Bell nonlocality [24–29]. These studies have indicated that sequential measurement scenarios provide an advantage in probing the maximum number of observers who can simultaneously demonstrate nonlocality, thereby implying potential applications in quantum networks. The goal of a quantum network is to achieve information transmission and secure communication between large-scale users. Based on suitable network Bell inequalities and an appropriate measurement strategy, network nonlocality can be revealed by all quantum nodes, with only a single observer per node in the original network. Network nonlocality sharing explores whether all observers in a generalized network scenario, which sequentially adds extra observers to some nodes in the original scenario, can simultaneously share nonlocality. In 2022 network nonlocality sharing based on two-sided sequential measurements in the bilocal scenario was first discussed in Ref. [30]. Subsequently, Wang *et al.* [31] explored a scenario involving n-sided sequential measurements in n-local star-shaped networks. Mahato *et al.* [32] showed that an alternative form of inequality could achieve the same effect, allowing an unbounded number of sequential observers to share star-shaped network nonlocality in a one-sided sequential measurement scenario. The scenario wherein an arbitrary number of sequential observers can

*Contact author: gfenzhuo@bupt.edu.cn

 ©2024 American Physical Society

participate on each of any m sides was established in Ref. [33]. More recently, Mao *et al.* [34] experimentally realized a star-shaped network nonlocality sharing protocol.

Apart from star-shaped networks, the tree-shaped network is another kind of quantum network generalized from the bilocal network. A tree-shaped network may show an advantage over a star-shaped network for some problems, such as time-evolution methods [35] and stochastic methods for open quantum systems [36]. In 2021 Yang *et al.* [16] initially introduced nonlinear Bell-type inequalities and confirmed the presence of network nonlocality in the tree-shaped network. However, it remains unclear whether sequential measurements can contribute to expanding the scale of the tree-shaped network. We investigate network nonlocality sharing in the two-forked n-layer ($n \geqslant 2$) tree-shaped network through multiple violations of the (2^n-2)-local inequality [16]. Such a network features (2^n-2) independent sources and (2^n-1) nodes. The uth $(1 \leqslant u \leqslant n)$ layer contains 2^{u-1} nodes. For the first $n-1$ layers, each node shares two different sources with two nodes in the next layer, respectively. Our findings indicate that for a sufficiently large value of n, an unbounded number of sequential observers on each sequential side can share the non-(2^n-2)-locality in any m-sided sequential measurement scenario. Furthermore, when n is finite, the study obtains a series of ranges about m in which one can directly obtain how many observers can share the non-(2^n-2)-locality per sequential side. For the simplest two-forked tree-shaped network (i.e., $n=3$), the sharing of the non-6-locality is demonstrated through four different cases. From one-sided to four-sided sequential measurement scenarios, it is respectively shown that at most 30, 6, 3, and 2 sequential observers on each sequential side can share the non-6-locality.

The structure of the paper is as follows: In Sec. II we review the description of the two-forked n-layer tree-shaped network. Subsequently, the network nonlocality sharing in the two-forked n-layer tree-shaped network is completely analyzed in Sec. III. We demonstrate the network nonlocality sharing in the two-forked three-layer tree-shaped network, as shown in Sec. IV. We end the paper with a conclusion in Sec. V.

II. PRELIMINARIES: THE TWO-FORKED *N*-LAYER TREE-SHAPED NETWORK

As depicted in Fig. 1, we consider a two-forked n-layer tree-shaped network for any $n \geqslant 2$, composed of 2^n-2 independent sources and 2^n-1 nodes. The 2^n-1 nodes are denoted by Alice^{11} (A^{11}), Alice^{21} (A^{21}), Alice^{22} (A^{22}), $\ldots$, Alice^{n1} (A^{n1}), $\ldots$, Alice$^{n2^{n-1}}$ ($A^{n2^{n-1}}$), where the superscript indicates every node's location. Denote the binary input and output of Alice^{uv} ($u=1,2,\ldots,n; v=1,2,\ldots,2^{u-1}$) by $x^{uv} \in \{0,1\}$ and $a^{uv} \in \{0,1\}$, respectively. All the 2^n-2 sources are characterized by independent hidden variable $\lambda_1,\ldots,\lambda_{2^n-2}$, respectively. The joint probability of all 2^n-1 nodes can be written in the following factorized form:

$$
\begin{aligned}
&P\big(a^{11}, a^{21}, a^{22}, a^{31}, \ldots, a^{n1}, \ldots, a^{n2^{n-1}} \big| x^{11}, x^{21}, x^{22}, x^{31}, \ldots, x^{n1}, \ldots, x^{n2^{n-1}}\big)\\
&\quad = \int \cdots \int d\lambda_1 \ldots d\lambda_{2^n-2} P(\lambda_1, \ldots, \lambda_{2^n-2}) \big[P(a^{11} \mid x^{11}, \lambda_1, \lambda_2) P(a^{21} | x^{21}, \lambda_1, \lambda_3, \lambda_4) P(a^{22} \mid x^{22}, \lambda_2, \lambda_5, \lambda_6) \ldots\\
&\quad \times P(a^{n1} \mid x^{n1}, \lambda_{2^{n-1}-1}) \ldots P\big(a^{n2^{n-1}} \mid x^{n2^{n-1}}, \lambda_{2^n-2}\big)\big]. \qquad (1)
\end{aligned}
$$

where $P(\lambda_1,\ldots,\lambda_{2^n-2})$ is a probability distribution over $\lambda_1,\ldots,\lambda_{2^n-2}$.

Since all the sources are independent of each other, probability distribution $P(\lambda_1,\ldots,\lambda_{2^n-2})$ can be written as

$$
P(\lambda_1, \ldots, \lambda_{2^n-2}) = P(\lambda_1) \ldots P(\lambda_{2^n-2}), \qquad (2)
$$

where $\int d\lambda_l P(\lambda_l) = 1, l = 1,2,\ldots,2^n-2$. The (2^n-1)-partite correlations are (2^n-2)-local if they satisfy the decomposition of Eq. (1) along with the constraint of Eq. (2). The correlation in terms of the probability distribution can be given as

$$
\big\langle A^{11}_{x^{11}} \ldots A^{n2^{n-1}}_{x^{n2^{n-1}}} \big\rangle = \sum_{a^{11},\ldots,a^{n2^{n-1}}} (-1)^{a^{11}+a^{21}+\cdots+a^{n2^{n-1}}} P\big(a^{11}, \ldots, a^{n2^{n-1}} \big| x^{11}, \ldots, x^{n2^{n-1}}\big), \qquad (3)
$$

where $A^{uv}_{x^{uv}}$ denotes the operator of Alice^{uv} with binary inputs x^{uv}, $u \in \{1,2,\ldots,n\}$, $v \in \{1,2,\ldots,2^{u-1}\}$. To verify non-$(2^n-2)$-locality, Yang *et al.* [16] introduced a set of Bell-type inequalities:

$$
S_{(2^n-2)-\mathrm{local}} = \sqrt[2^{n-1}]{\big|I_{i_1,\ldots,i_{2^{n-1}-1},0}\big|} + \sqrt[2^{n-1}]{\big|I_{j_1,\ldots,j_{2^{n-1}-1},1}\big|} \leqslant 1, \qquad (4)
$$

where

$$
I_{i_1(j_1),\ldots,i_{2^{n-1}-1}(j_{2^{n-1}-1}),t} = \frac{1}{2^{2^{n-1}}} \sum_{x^{n1},\ldots,x^{n2^{n-1}}} (-1)^{t*(x^{n1}+\cdots+x^{n2^{n-1}})} \big\langle A^{11}_{i_1(j_1)} \ldots A^{n2^{n-1}}_{x^{n2^{n-1}}} \big\rangle, \qquad (5)
$$

$i_r, j_r \in \{0,1\}$, $r \in \{1,\ldots,2^{n-1}-1\}$, and $t \in \{0,1\}$.

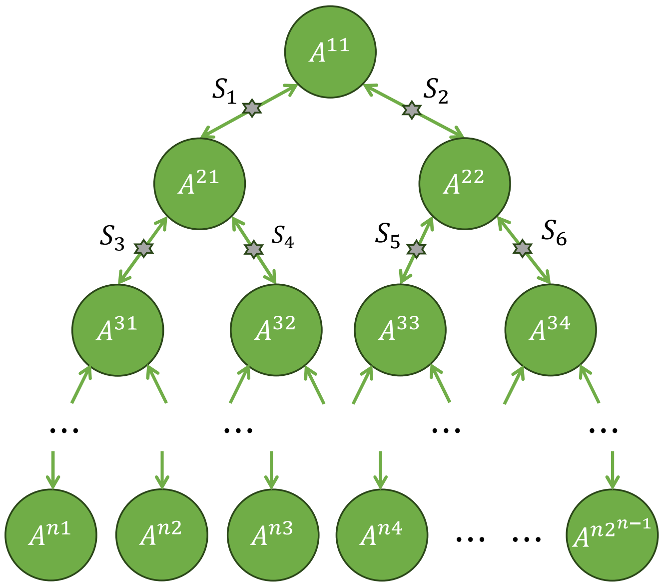

FIG. 1. The two-forked n-layer tree-shaped network is composed of 2^n-2 independent sources and 2^n-1 nodes. The 2^n-1 nodes are distributed into n ($n\geqslant 2$) layers. The superscript uv in Alice^{uv} indicates the vth node on the uth layer ($1\leqslant u\leqslant n$). There exist 2^{u-1} nodes on the uth layer. For the first $n-1$ layers, each node respectively shares two different sources with two nodes in the next layer.

Violating at least one possible inequality of Eq. (4) guarantees the corresponding non-(2^n-2)-locality. Taking $i_r=0, j_r=1$ for $r=1,\dots,2^{n-1}-1$, then inequality (4) becomes the following form:

$$S_{(2^n-2)-\text{local}}=\sqrt[2^{n-1}]{|I_{0,\dots,0}|}+\sqrt[2^{n-1}]{|I_{1,\dots,1}|}\leqslant 1. \tag{6}$$

Assuming that each source produces a maximally entangled two-qubit state, the optimal quantum violation of $S_{(2^n-2)-\text{local}}$ in Eq. (6) is $\sqrt{2}$, which can be obtained by the following measurement strategy:

$$A_0^{11}=\sigma_z\otimes\sigma_z,\quad A_0^{uv}=\sigma_z\otimes\sigma_z\otimes\sigma_z,\quad A_0^{ni}=\frac{\sigma_z+\sigma_x}{\sqrt{2}},$$
$$A_1^{11}=\sigma_x\otimes\sigma_x,\quad A_1^{uv}=\sigma_x\otimes\sigma_x\otimes\sigma_x,\quad A_1^{ni}=\frac{\sigma_z-\sigma_x}{\sqrt{2}}, \tag{7}$$

where $u\in\{2,3,\dots,n-1\}$, $v\in\{1,2,\dots,2^{u-1}\}$, and $i\in\{1,2,\dots,2^{n-1}\}$.

III. NETWORK NONLOCALITY SHARING IN THE N-LAYER TREE-SHAPED NETWORK

The scenario depicted in Fig. 2 is considered, where 2^n-2 independent sources emit the state $\rho_{A^{11}A^{21}}$, $\rho_{A^{11}A^{22}}$, $\dots$, $\rho_{A^{(n-1)1}A^{n1}}$, $\dots$, $\rho_{A^{(n-1)2^{n-2}}A^{n2^{n-1}}}$, respectively. Then the overall quantum state has the following form:

$$\rho=\rho_{A^{11}A^{21}}\otimes\cdots\otimes\rho_{A^{(n-1)1}A^{n1}}\otimes\cdots\otimes\rho_{A^{(n-1)2^{n-2}}A^{n2^{n-1}}}. \tag{8}$$

Suppose that there are k observers on Alice^{ni}'s side for $i\in\{1,\dots,2^{n-1}\}$, which are denoted by Alice$_1^{ni}$ (A_1^{ni}), Alice$_2^{ni}$ (A_2^{ni}), $\dots$, Alice$_k^{ni}$ (A_k^{ni}), respectively. On each Alice^{ni}'s side, Alice$_1^{ni}$ performs the measurement $A^{ni}_{1,x_1^{ni}}$ according to her measurement choices $x_1^{ni}(\in\{0,1\})$ and records the outcomes $a_1^{ni}(\in\{0,1\})$. The postmeasurement state is then sent to Alice$_2^{ni}$. Using the Lüders rule, the state shared between Alice^{11}, $\dots$, Alice$^{(n-1)2^{n-2}}$, Alice$_2^{n1}$, $\dots$, Alice$_2^{n2^{n-1}}$ is given by

$$\rho^{(2,\dots,2)}=\frac{1}{2^{2^{n-1}}}\sum_{\substack{a_1^{n1},\dots,a_1^{n2^{n-1}}\\ x_1^{n1},\dots,x_1^{n2^{n-1}}}}(\mathcal{M}_I\otimes\mathcal{N}_1)^\dagger\rho^{(1,\dots,1)}(\mathcal{M}_I\otimes\mathcal{N}_1), \tag{9}$$

where

$$\mathcal{M}_I=(I\otimes I)\otimes(I\otimes I\otimes I)\otimes\cdots\otimes(I\otimes I\otimes I),$$
$$\mathcal{N}_1=\Big(I\otimes\sqrt{A^{n1}_{1,a_1^{n1}|x_1^{n1}}}\Big)\otimes\cdots\otimes\Big(I\otimes\sqrt{A^{n2^{n-1}}_{1,a_1^{n2^{n-1}}|x_1^{n2^{n-1}}}}\Big), \tag{10}$$

and $\rho^{(1,\dots,1)}$ is the initial state ρ, $A^{ni}_{1,a_1^{ni}|x_1^{ni}}$ is the positive operator-valued measure (POVM) element corresponding to the outcome a_1^{ni} of Alice$_1^{ni}$'s measurement for the input x_1^{ni}, and I is the 2×2 identity matrix.

After a direct calculation, we have

$$\rho^{(2,\dots,2)}=\rho_{A^{11}A^{21}}\otimes\cdots\otimes\rho_{A^{(n-2)2^{n-3}}A^{(n-1)2^{n-2}}}\bigotimes_{s=1}^{2^{n-2}}\left(\bigotimes_{i=2s-1}^{2s}\rho^{(2)}_{A^{(n-1)s}A^{ni}}\right), \tag{11}$$

where

$$\rho^{(2)}_{A^{(n-1)s}A^{ni}}=\frac{1}{2}\sum_{a_1^{ni},x_1^{ni}}\Big(I\otimes\sqrt{A^{ni}_{1,a_1^{ni}|x_1^{ni}}}\Big)\rho^{(1)}_{A^{(n-1)s}A^{ni}}\Big(I\otimes\sqrt{A^{ni}_{1,a_1^{ni}|x_1^{ni}}}\Big). \tag{12}$$

Repeating this process, the state shared between Alice^{11}, $\dots$, Alice$^{(n-1)2^{n-2}}$, Alice$_k^{n1}$, $\dots$, Alice$_k^{n2^{n-1}}$ can be represented as

$$\rho^{(k,\dots,k)}=\rho_{A^{11}A^{21}}\otimes\cdots\otimes\rho_{A^{(n-2)2^{n-3}}A^{(n-1)2^{n-2}}}\bigotimes_{s=1}^{2^{n-2}}\left(\bigotimes_{i=2s-1}^{2s}\rho^{(k)}_{A^{(n-1)s}A^{ni}}\right), \tag{13}$$

where

$$\rho^{(k)}_{A^{(n-1)s}A^{ni}} = \frac{1}{2}\sum_{a^{ni}_{k-1},x^{ni}_{k-1}} \left(I\otimes\sqrt{A^{ni}_{k-1,a^{ni}_{k-1}|x^{ni}_{k-1}}}\right)\rho^{(k-1)}_{A^{(n-1)s}A^{ni}}\left(I\otimes\sqrt{A^{ni}_{k-1,a^{ni}_{k-1}|x^{ni}_{k-1}}}\right). \tag{14}$$

In the whole process, Alice$^{ni}_j$ acts independently of the previous observers in this sequence, and the measurement choices of Alice$^{ni}_1, \ldots,$ Alice$^{ni}_k$ are completely unbiased.

Since a projective measurement destroys the state maximally, the postmeasurement state is unentangled [24]. To achieve an optimal trade-off between measurement disturbance and information gain, the unsharp measurement [25] is considered, which is a particular kind of POVM. We employ the dichotomic POVMs with measurement operators $\{E, I-E\}$, where $E = \frac{1}{2}(I+\gamma\sigma_{\vec{r}})$, $\vec{r} = (r_1, r_2, r_3) \in \mathbb{R}^3$ with $\|\vec{r}\| = 1$, $\gamma \in [0, 1]$ is the sharpness parameter, and $\sigma_{\vec{r}} = r_1\sigma_x + r_2\sigma_y + r_3\sigma_z$.

Our measurement strategy of Alice on the first $n-1$ layers is the same as Eq. (7). On each Alice^{ni}'s ($i \in \{1, \ldots, 2^{n-1}\}$) side, each Alice$^{ni}_j$ except the final Alice$^{ni}_k$ performs unsharp measurements. Alice$^{ni}_j$'s POVMs are defined as

$$\begin{aligned} A^{ni}_{j,0|0} &= \frac{1}{2}\left(I + \frac{\gamma^{ni}_j}{\sqrt{2}}[\sigma_z + \sigma_x)\right], \\ A^{ni}_{j,0|1} &= \frac{1}{2}\left(I + \frac{\gamma^{ni}_j}{\sqrt{2}}[\sigma_z - \sigma_x)\right], \end{aligned} \tag{15}$$

where $\gamma^{ni}_j \in [0, 1]$ ($i \in \{1, 2, \ldots, 2^{n-1}\}$, $j \in \{1, 2, \ldots, k\}$) denotes the sharpness parameter of Alice$^{ni}_j$. Further, the expectation operators are given by $A^{ni}_{j,x^{ni}_j} = A^{ni}_{j,0|x^{ni}_j} - A^{ni}_{j,1|x^{ni}_j}$ for $x^{ni}_j \in \{0, 1\}$. Using these measurements, the expected value of $S^{(k,\ldots,k)}_{(2^n-2)-\text{local}}$ among Alice$^{11}, \ldots,$ Alice$^{(n-1)2^{n-2}}$, Alice$^{n1}_k, \ldots,$ Alice$^{n2^{n-1}}_k$ is obtained.

Theorem 1. For the initial overall quantum state $\rho^{(1,\ldots,1)} = \rho_{A^{11}A^{21}} \otimes \rho_{A^{11}A^{22}} \otimes \cdots \otimes \rho_{A^{(n-1)1}A^{n1}} \otimes \cdots \otimes \rho_{A^{(n-1)2^{n-2}}A^{n2^{n-1}}}$, where $\rho_{A^{11}A^{21}} = \cdots = \rho_{A^{(n-1)2^{n-2}}A^{n2^{n-1}}} = |\psi\rangle\langle\psi|$, $|\psi\rangle = \frac{|00\rangle+|11\rangle}{\sqrt{2}}$, the expected value of $S^{(k,\ldots,k)}_{(2^n-2)-\text{local}}$ associated with the state $\rho^{(k,\ldots,k)}$ is given by

$$S^{(k,\ldots,k)}_{(2^n-2)-\text{local}} = \sqrt{2}\,\sqrt[2^{n-1}]{\prod_{i=1}^{2^{n-1}}\left(\gamma^{ni}_k\prod_{j=1}^{k-1}\frac{1+\sqrt{1-\left(\gamma^{ni}_j\right)^2}}{2}\right)}, \tag{16}$$

where $\gamma^{ni}_j \in [0, 1]$ is the sharpness parameter of Alice$^{ni}_j$. The proof is given in the Appendix.

In what follows, we consider the m-sided ($1 \leqslant m \leqslant 2^{n-1}$) sequential measurement case where m denotes the number of S nodes. We can assume without loss of generality that Alice^{ni} (Alice$^{ni}_1$, $i \in \{1, \ldots, m\}$) is an S node, and there are multiple sequential observers (Alice$^{ni}_k$) who perform unsharp measurements on each Alice^{ni}'s side. The Alice^{nl} (Alice$^{nl}_1$, $l \in \{m+1, \ldots, 2^{n-1}\}$) and all the nodes on the first $n-1$ layers are non-S nodes. Hence, Alice^{nl} ($l \in \{m+1, \ldots, 2^{n-1}\}$) performs projective measurements, i.e., $\gamma_1^{n(m+1)} = \cdots = \gamma_1^{n2^{n-1}} = 1$. Consequently, the expected value of $S^{(k,\ldots,k)}_{(2^n-2)-\text{local}}$ can be rewritten as

$$S^{(\overbrace{k,\ldots,k}^{m},1,\ldots,1)}_{(2^n-2)-\text{local}} = \sqrt{2}\,\sqrt[2^{n-1}]{\prod_{i=1}^{m}\left(\gamma^{ni}_k\prod_{j=1}^{k-1}\frac{1+\sqrt{1-\left(\gamma^{ni}_j\right)^2}}{2}\right)}. \tag{17}$$

For simplicity, when $\gamma^{n1}_j = \gamma^{n2}_j = \cdots = \gamma^{nm}_j = \gamma_j$, Eq. (17) reduces to

$$S^{(k,\ldots,k,1,\ldots,1)}_{(2^n-2)-\text{local}} = \sqrt{2}\left(\gamma_k\prod_{j=1}^{k-1}\frac{1+\sqrt{1-\gamma_j^2}}{2}\right)^{\frac{m}{2^{n-1}}}. \tag{18}$$

To ensure the arbitrary kth observer per S node can share the non-(2^n-2)-locality with all non-S nodes. It is sufficient

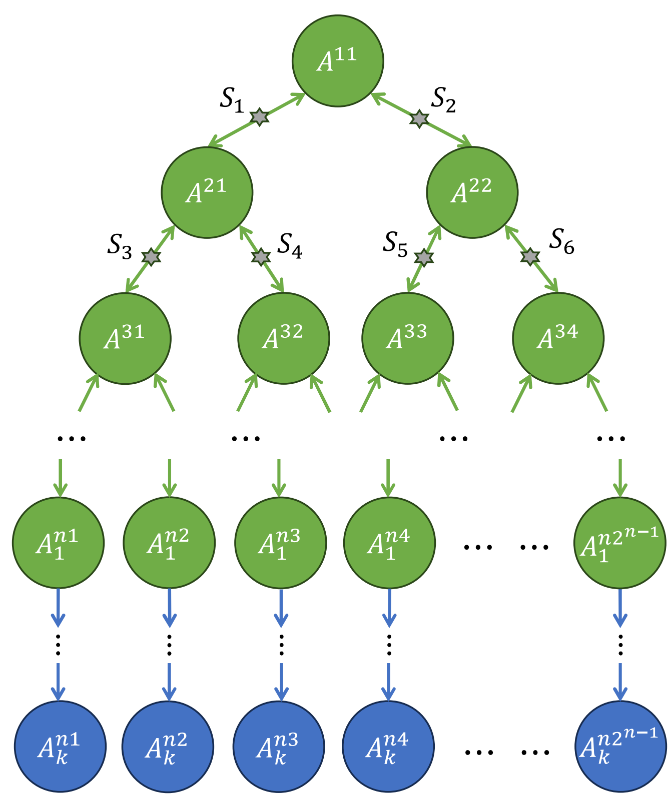

FIG. 2. Network nonlocality sharing under 2^{n-1}-sided sequential measurements in the two-forked n-layer tree-shaped network. For simplicity, the green nodes on the nth layer that have multiple sequential blue observers are labeled as S nodes, while any other green nodes are labeled as non-S nodes. Since there exist k sequential observers on each Alice^{ni}'s side, Alice^{ni} (Alice$^{ni}_1$) is an S node for $i = 1, 2, \ldots, 2^{n-1}$.

to choose appropriate values of γ_j such that $S^{(j,\ldots,j,1,\ldots,1)}_{(2^n-2)-\text{local}} > 1$ holds for all $j \in \{1,\ldots,k\}$. From Eq. (18), we thus deduce

$$\gamma_1 > 2^{-\frac{2^{n-2}}{m}}, \tag{19a}$$

$$\gamma_j > \frac{2\gamma_{j-1}}{1+\sqrt{1-\gamma_{j-1}{}^2}}, \quad j = 2,\ldots,k. \tag{19b}$$

Note that the inequality $1+\sqrt{1-\gamma_j{}^2} \geqslant 2\sqrt{1-\gamma_j{}^2}$ holds for any $\gamma_j \in [0,1]$, Applied it to Eqs. (19), we obtain

$$\gamma_j > \frac{\gamma_{j-1}}{\sqrt{1-\gamma_{j-1}{}^2}}, j = 2,\ldots,k. \tag{20}$$

For $j = 2$,

$$\gamma_2 > \frac{\gamma_1}{\sqrt{1-\gamma_1{}^2}} = \frac{1}{\sqrt{\frac{1}{\gamma_1^2}-1}} > \frac{1}{\sqrt{2^{\frac{2^{n-1}}{m}}-1}}. \tag{21}$$

Repeating this process, we obtain the lower bound of sharpness parameter γ_k for the kth sequential observer

$$\gamma_k > \frac{1}{\sqrt{2^{\frac{2^{n-1}}{m}}-(k-1)}}. \tag{22}$$

Note further that the lower bound of sharpness parameter γ_k holds for a suitable n, the inequality (22) can be rewritten as

$$2^{n-1} > m\log_2\left(k-1+\frac{1}{\gamma_k^2}\right). \tag{23}$$

If the kth sequential observer performs projective measurements, i.e., $\gamma_k = 1$, we have

$$2^{n-1} > m\log_2 k. \tag{24}$$

For any given m and k, there may be a suitable n that satisfies Eq. (24). That is to say, in any m-sided sequential measurement scenario, there exists a suitable n such that the kth sequential observer on each of m sides can share the non-(2^n-2)-locality with all non-S nodes. Hence, when n is arbitrarily large, k is unbounded. We also find that when n is fixed, the smaller m indicates the greater k.

Since the lower bound of γ_k, which depends on n and m, in Eq. (22) is an approximate solution, it is interesting to explore the direct relationship among k, m, and n. We define the critical value γ_j^* of the sharpness parameter γ_j, which is the maximum value that satisfies the inequality $S^{(j,\ldots,j,1,\ldots,1)}_{(2^n-2)-\text{local}} \leqslant 1$ for all $j \in \{1,\ldots,k\}$. Then $S^{(j,\ldots,j,1,\ldots,1)}_{(2^n-2)-\text{local}} > 1$ as long as $\gamma_j > \gamma_j^*$.

Taking $x = 2^{-\frac{2^{n-2}}{m}}$ $(0 < x \leqslant \frac{1}{\sqrt{2}})$, we will discuss the specific value of k for different ranges of x.

(1) $k = 2$, i.e., there are at most two sequential observers on each of m sides. Let us consider the critical values of γ_1, γ_2, and γ_3. Using Eqs. (19) for $k = 3$, we have

$$\gamma_1^* = x_2,$$
$$\gamma_{q+1}^* = \frac{2\gamma_q^*}{1+\sqrt{1-\gamma_q^{*2}}}, \quad q \in \{1,2\}. \tag{25}$$

As shown in Fig. 3(a), taking $x_1 = \frac{1}{\sqrt{2}}$, both γ_1^* and γ_2^* are less than 1 for all $x \in (0, x_1]$. Hence, there are at least two sequential observers per sequential side. As illustrated in Fig. 3(b), when $\gamma_3^* = 1$, we obtain $\gamma_2^* = 0.8$, $\gamma_1^* = 0.6897$, and $x_2 = \gamma_1^* = 0.6897$. As γ_3^* is a monotonically increasing function of x, when $x \geqslant x_2$, γ_3^* is an invalid value, i.e., $\gamma_3^* \geqslant 1$. Therefore, for all $x \in [x_2, x_1]$, there are at most two sequential observers per sequential side.

(2) $k = 3$, i.e., there are at most three observers on each of m sides. Let us consider the critical values of γ_1, γ_2, γ_3, and γ_4. Using Eqs. (19) for $k = 4$, we have

$$\gamma_1^* = x_3,$$
$$\gamma_{q+1}^* = \frac{2\gamma_q^*}{1+\sqrt{1-\gamma_q^{*2}}}, \quad q \in \{1,2,3\}. \tag{26}$$

As shown in Fig. 3(b), for any $x < x_2$, γ_1^*, γ_2^*, and γ_3^* are less than 1. It implies that there are at least three sequential observers per sequential side for $x \in (0, x_2)$. When $\gamma_4^* = 1$, we

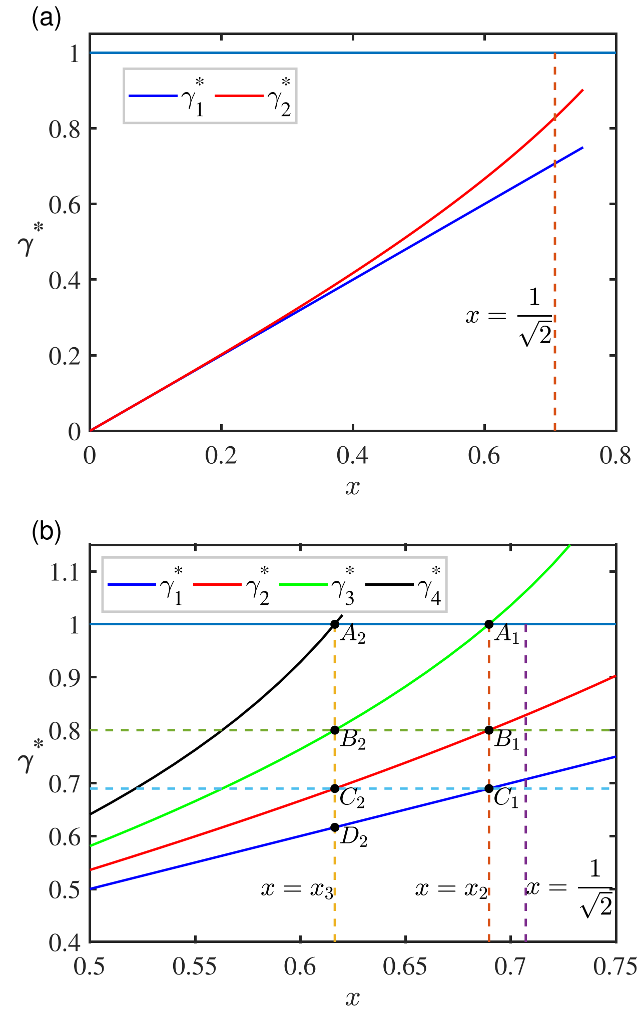

FIG. 3. Critical values of sharpness parameters of sequential observers on each side required for violating the (2^n-2)-local inequality. (a) Plot of γ_1^* and γ_2^* with blue and red lines, respectively. (b) Plot of γ_1^*, γ_2^*, γ_3^*, and γ_4^*, with blue, red, green, and black lines, respectively. Points A_1, B_1, and C_1 represent the intersection points of γ_3^*, γ_2^*, and γ_1^*, respectively, and $x = x_2$. Points A_2, B_2, C_2, and D_2 represent the intersection points of γ_4^*, γ_3^*, γ_2^*, and γ_1^*, respectively, and $x = x_3$.

TABLE I. Ranges of $m(n)$ for any k, where $m(\in \mathbb{N}^+)$ is the number of S nodes. For a fixed k and n, the range of m may not include a positive integer; it implies that the number k of sequential observers can be achieved by the positive integer obtained by rounding down the lower bound of the range.

k	m
2	$2.0000 \times 2^{n-2} \geqslant m \geqslant 1.8655 \times 2^{n-2}$
3	$1.8655 \times 2^{n-2} > m \geqslant 1.4324 \times 2^{n-2}$
4	$1.4324 \times 2^{n-2} > m \geqslant 1.2062 \times 2^{n-2}$
5	$1.2062 \times 2^{n-2} > m \geqslant 1.0649 \times 2^{n-2}$
6	$1.0649 \times 2^{n-2} > m \geqslant 0.9672 \times 2^{n-2}$
7	$0.9672 \times 2^{n-2} > m \geqslant 0.8948 \times 2^{n-2}$
8	$0.8948 \times 2^{n-2} > m \geqslant 0.8388 \times 2^{n-2}$
9	$0.8388 \times 2^{n-2} > m \geqslant 0.7939 \times 2^{n-2}$
10	$0.7939 \times 2^{n-2} > m \geqslant 0.7569 \times 2^{n-2}$
...	...
29	$0.5075 \times 2^{n-2} > m \geqslant 0.5016 \times 2^{n-2}$
30	$0.5016 \times 2^{n-2} > m \geqslant 0.4960 \times 2^{n-2}$
31	$0.4960 \times 2^{n-2} > m \geqslant 0.4906 \times 2^{n-2}$
...	...

have $\gamma_3^* = 0.8$, $\gamma_2^* = 0.6897$, $\gamma_1^* = 0.6164$, and $x_3 = 0.6164$. When $x \geqslant x_3$, γ_4^* is an invalid value, i.e., $\gamma_4^* \geqslant 1$. Similarly, for all $x \in [x_3, x_2)$, there are at most three sequential observers on each of m sides.

(3) Repeating this procedure, we obtain a sequence of x_k, $k \in \{1, 2, 3, \ldots\}$ in the following:

$$x_1 = 0.7071,$$
$$x_2 = 0.6897,$$
$$x_k = \frac{4x_{k-1}}{4 + {x_{k-1}}^2}, \quad k = 3, \ldots. \tag{27}$$

When $x \in [x_k, x_{k-1})$, there are at most k observers per sequential side. Since $x = 2^{-\frac{2^{n-2}}{m}}$, we get $m = -\frac{2^{n-2}\log 2}{\log x}$, the direct relationship among k, m, and n. As shown in Table I, given a finite n, we can explicitly obtain the number k of sequential observers for different m-sided cases.

When $n = 2$, as illustrated in Table II, we have the following: (1) When $m = 2$, there are at most two observers. (2) When $m = 1$, there are at most six observers. This is coincident with the result derived in Refs. [30,32]. For the case of $k = 7$, the range of m does not include a positive integer. Then the lower bound 0.8948 rounds down to 0. This implies that network nonlocality cannot be shared under one-sided and two-sided sequential measurements.

TABLE II. Ranges of m for any k when $n = 2$.

k	m
2	$2.0000 \geqslant m \geqslant 1.8655$
3	$1.8655 > m \geqslant 1.4324$
4	$1.4324 > m \geqslant 1.2062$
5	$1.2062 > m \geqslant 1.0649$
6	$1.0649 > m \geqslant 0.9672$
7	$0.9672 > m \geqslant 0.8948$

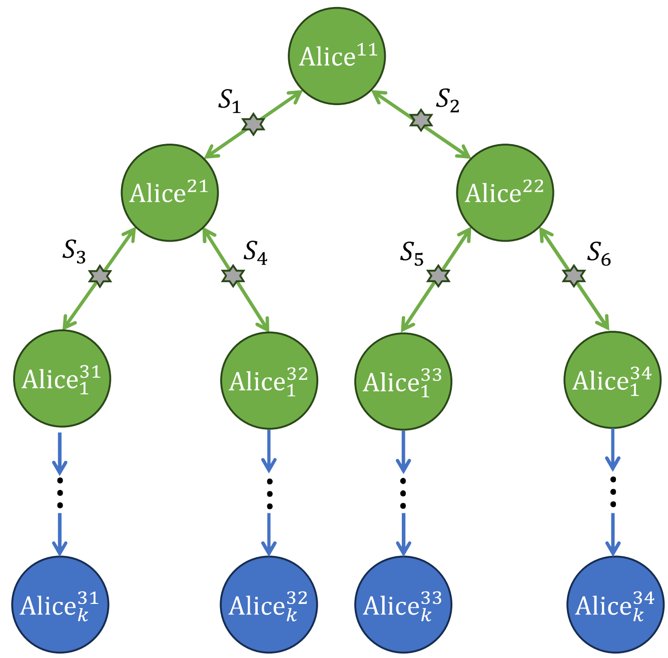

FIG. 4. Network nonlocality sharing under four-sided sequential measurements in the two-forked three-layer tree-shaped network. There exist k sequential observers on Alice^{3i}'s side for $i \in \{1, 2, 3, 4\}$. Each Alice$_j^{3i}$, $j \in \{1, \ldots, k-1\}$ performs unsharp measurements, and Alice$_k^{3i}$ performs projective measurements.

IV. NETWORK NONLOCALITY SHARING IN THE THREE-LAYER TREE-SHAPED NETWORK

To further illustrate our results for a finite n, we consider network nonlocality sharing in the two-forked three-layer tree-shaped network, which is composed of seven spatially separated nodes (Alice^{11}, Alice^{21}, Alice^{22}, Alice^{31}, Alice^{32}, Alice^{33}, Alice^{34}) and six sources ($S_1, S_2, S_3, S_4, S_5, S_6$), as illustrated in Fig. 4. Alice^{3i} (Alice$_1^{3i}$, $i \in \{1, 2, 3, 4\}$) is an S node, while Alice^{11}, Alice^{21}, and Alice^{22} are non-S nodes. Multiple independent Alice^{3i}s (say, Alice$_1^{3i}, \ldots,$ Alice$_k^{3i}$) measure their shared qubit sequentially for $i = 1, 2, 3, 4$.

Similarly to Theorem 1, we can obtain the expected value of $S_{6-\text{local}}^{(k,k,k,k)}$.

Corollary 1. For the initial state $\rho^{(1,1,1,1)} = \rho_{AB^1} \otimes \rho_{AB^2} \otimes \rho_{B^1C^1} \otimes \rho_{B^1C^2} \otimes \rho_{B^2C^3} \otimes \rho_{B^2C^4}$, where $\rho_{AB^1} = \rho_{AB^2} = \rho_{B^1C^1} = \rho_{B^1C^2} = \rho_{B^2C^3} = \rho_{B^2C^4} = |\psi\rangle\langle\psi|$, $|\psi\rangle = \frac{|00\rangle + |11\rangle}{\sqrt{2}}$, the expected $S_{6-\text{local}}$ value of $\rho^{(k,k,k,k)}$ is given by

$$S_{6-\text{local}}^{(k,k,k,k)} = \sqrt{2}\sqrt[4]{\prod_{i=1}^{4}\left(\gamma_k^{3i}\prod_{j=1}^{k-1}\frac{1+\sqrt{1-(\gamma_j^{3i})^2}}{2}\right)}. \tag{28}$$

In the four-sided sequential measurement scenario, we assume that $\gamma_j^{31} = \gamma_j^{32} = \gamma_j^{33} = \gamma_j^{34} = \gamma_j$, $j \in \{1, \ldots, k\}$. To find γ_j and the maximum value of k for the number of sequential observers such that $S_{6-\text{local}}^{(j,j,j,j)} > 1$ for all $j \in \{1, \ldots, k\}$

TABLE III. Ranges of m for any k when $n = 3$.

k	m
2	$4.0000 \geqslant m \geqslant 3.7310$
3	$3.7310 > m \geqslant 2.8648$
4	$2.8648 > m \geqslant 2.4124$
5	$2.4124 > m \geqslant 2.1298$
6	$2.1298 > m \geqslant 1.9344$
7	$1.9344 > m \geqslant 1.7896$
…	…
29	$1.0150 > m \geqslant 1.0032$
30	$1.0032 > m \geqslant 0.9920$
31	$0.9920 > m \geqslant 0.9812$
…	…

is necessary. From Eq. (28), we obtain

$$\gamma_1 > \frac{1}{\sqrt{2}},$$
$$\gamma_j > \frac{2\gamma_{j-1}}{1+\sqrt{1-\gamma_{j-1}^2}}, j = 2, \dots, k. \tag{29}$$

The critical values of γ_1, γ_2, and γ_3 are $\gamma_1^* = 0.7071$, $\gamma_2^* = 0.8284$, and $\gamma_3^* = 1.0620$, respectively. This implies that at most two sequential observers on each Alice^{3i} ($i = 1, 2, 3, 4$) side can share the non-6-locality through the violation of the 6-local inequality in Eq. (6) with all non-S nodes. In the m-sided ($m = 1, 2, 3$) sequential measurement case, Alice^{31}, …, Alice^{3m} are S nodes, while all other nodes are non-S nodes. Similarly, we can obtain the first invalid value in the m-sided ($m = 1, 2, 3$) cases, respectively: (1) $m = 3$, $\gamma_4^* = 1.0699$; (2) $m = 2$, $\gamma_7^* = 1.1354$; (3) $m = 1$, $\gamma_{31}^* = 1.3574$. This implies that at most 3, 6, and 30 sequential observers on each S node can share the non-6-locality through the violation of the 6-local inequality in Eq. (6) with all non-S nodes in three-sided, two-sided, and one-sided cases, respectively.

As illustrated in Table III, when $n = 3$, the above result of network nonlocality sharing in the two-forked three-layer tree-shaped network can be directly obtained.

V. CONCLUSION

As a powerful resource in quantum networks, network nonlocality has been applied in various information processing tasks. Unlike the typical Bell scenario, the set of local correlations in the network is nonconvex, rendering the detection and sharing of network nonlocality more challenging. In this work, the phenomenon of quantum network nonlocality sharing in the two-forked n-layer tree-shaped network via arbitrary m-sided ($m \in \{1, 2, \dots, 2^{n-1}\}$) sequential measurements has been discussed.

In the general case involving n layers, given an arbitrary m there exists a suitable n that enables a maximum value of $k(n, m)$ independent observers per sequential side to share the non-($2^n - 2$)-locality. Especially, when n is sufficiently large, an unbounded number of independent observers per sequential side can simultaneously share the non-($2^n - 2$)-locality. When n is finite, we have respectively obtained a range of m for any $k \in \{2, 3, \dots\}$. This allows for the direct determination of how many observers can share the non-($2^n - 2$)-locality when the values of n and m are known. In the simple special case of $n = 2$, our scenario backs to the bilocal scenario, and the result matches those in Refs. [30,32]. Furthermore, we can also provide distinct combinations of m and n for a specific number of observers.

To further illustrate our conclusion regarding the finite n situation, we have considered the case of $n = 3$ via arbitrary m-sided ($m = 1, 2, 3, 4$) sequential measurements, and demonstrated that the non-6-locality can be shared by, at most, 30, 6, 3, and 2 sequential observers on each sequential side, respectively. This indicates that as m increases, the quantity of sequential observers decreases.

Based on the premise that each source emits a maximally entangled two-qubit state, our work presents a framework for sharing network nonlocality within a two-forked tree-shaped network. Conceptually, our framework facilitates the analysis of nonlocality sharing in this network configuration, applicable to any pure or mixed two-qubit entangled state. It also enhances the generalization and realization of known applications found in typical nonlocality sharing scenarios, such as randomness certification.

The experimental demonstration of the nonlocality sharing has been realized by Hu *et al.* [37], which achieved double Bell inequality violations introduced in Ref. [23] under a state visibility of (99.70 ± 0.06) percent. Our research advances the implementation of network nonlocality sharing in two-forked tree-shaped networks. As our work incorporates much more observers, the visibility requirement may exceed 99.70%. This should be carefully considered for the subsequent verification experiment.

ACKNOWLEDGMENTS

This work is supported by the National Natural Science Foundation of China (Grants No. 62171056, No. 61973021, and No. 62220106012) and the Henan Key Laboratory of Network Cryptography Technology (Grant No. LNCT2022-A03).

APPENDIX: PROOF OF THEOREM 1

We provide detailed proof of Theorem 1, according to the expression of Eq. (6), the expected $S^{(k,\dots,k)}_{(2^n-2)-\mathrm{local}}$ value of $\rho^{(k,\dots,k)}$ can be given in the following:

$$S^{(k,\dots,k)}_{(2^n-2)-\mathrm{local}} = \sqrt[2^{n-1}]{\left|I^{(k,\dots,k)}_{0,\dots,0}\right|} + \sqrt[2^{n-1}]{\left|I^{(k,\dots,k)}_{1,\dots,1}\right|}, \tag{A1}$$

where

$$I_{0,\ldots,0}^{(k,\ldots,k)} = \frac{1}{2^{2^{n-1}}} \sum_{x^{n1},\ldots,x^{n2^{n-1}}} \langle A_0^{11} \ldots A_0^{(n-1)2^{n-2}} A_{x^{n1}}^{n1} \ldots A_{x^{n2^{n-1}}}^{n2^{n-1}} \rangle \tag{A2}$$

and

$$I_{1,\ldots,1}^{(k,\ldots,k)} = \frac{1}{2^{2^{n-1}}} \sum_{x^{n1},\ldots,x^{n2^{n-1}}} (-1)^{x^{n1}+\cdots+x^{n2^{n-1}}} \langle A_1^{11} \ldots A_1^{(n-1)2^{n-2}} A_{x^{n1}}^{n1} \ldots A_{x^{n2^{n-1}}}^{n2^{n-1}} \rangle. \tag{A3}$$

Next, using the state $\rho^{(k,\ldots,k)}$ in Eq. (13), the value of $I_{0,\ldots,0}^{(k,\ldots,k)}$ can be calculated:

$$\begin{aligned} I_{0,\ldots,0}^{(k,\ldots,k)} &= \frac{1}{2^{2^{n-1}}} \langle A_0^{11} \cdots A_0^{(n-1)2^{n-2}} \big(A_{k,0}^{n1} + A_{k,1}^{n1}\big) \cdots \big(A_{k,0}^{n2^{n-1}} + A_{k,1}^{n2^{n-1}}\big) \rangle \\ &= \frac{1}{2^{2^{n-1}}} \mathrm{Tr}[(\sigma_z \otimes \sigma_z)\rho_{A^{11}A^{21}}] \cdots \mathrm{Tr}[(\sigma_z \otimes \sigma_z)\rho_{A^{(n-2)2^{n-3}}A^{(n-1)2^{n-2}}}] \\ &\quad \times \prod_{s=1}^{2^{n-2}} \prod_{i=2s-1}^{2s} \mathrm{Tr}\big[\sigma_z \otimes \big(A_{k,0}^{ni} + A_{k,1}^{ni}\big)\rho_{A^{(n-1)s}A^{ni}}^{(k)}\big] \\ &= \frac{1}{2^{2^{n-1}}} \prod_{s=1}^{2^{n-2}} \prod_{i=2s-1}^{2s} \mathrm{Tr}\big[\sigma_z \otimes \big(A_{k,0}^{ni} + A_{k,1}^{ni}\big)\rho_{A^{(n-1)s}A^{ni}}^{(k)}\big]. \end{aligned} \tag{A4}$$

Now consider the quantity $\mathrm{Tr}[\sigma_z \otimes (A_{k,0}^{ni} + A_{k,1}^{ni})\rho_{A^{(n-1)s}A^{ni}}^{(k)}]$. Using Eq. (14) and the identity

$$\sqrt{A_{k-1,a_{k-1}^{ni}|x_{k-1}^{ni}}^{ni}} = \frac{1}{2\sqrt{2}}\Big(\sqrt{1+\gamma_{k-1}^{ni}} - \sqrt{1-\gamma_{k-1}^{ni}}\Big)I \;\; + \frac{1}{2\sqrt{2}}(-1)^{a_{k-1}^{ni}}\Big(\sqrt{1+\gamma_{k-1}^{ni}} - \sqrt{1-\gamma_{k-1}^{ni}}\Big)A_{x_{k-1}^{ni}}^{ni}, \tag{A5}$$

we can get

$$\begin{aligned} \mathrm{Tr}\big[\sigma_z \otimes \big(A_{k,0}^{ni} + A_{k,1}^{ni}\big)\rho_{A^{(n-1)s}A^{ni}}^{(k)}\big] &= \gamma_k^{ni} \mathrm{Tr}\big[\sigma_z \otimes \big(A_0^{ni} + A_1^{ni}\big)\rho_{A^{(n-1)s}A^{ni}}^{(k)}\big] \\ &= \gamma_k^{ni} \frac{1+\sqrt{1-\big(\gamma_{k-1}^{ni}\big)^2}}{2} \mathrm{Tr}\big[\sigma_z \otimes \big(A_0^{ni} + A_1^{ni}\big)\rho_{A^{(n-1)s}A^{ni}}^{(k-1)}\big]. \end{aligned} \tag{A6}$$

By recursion, we have

$$\begin{aligned} \mathrm{Tr}\big[\sigma_z \otimes \big(A_{k,0}^{ni} + A_{k,1}^{ni}\big)\rho_{A^{(n-1)s}A^{ni}}^{(k)}\big] &= \sqrt{2}\gamma_k^{ni} \prod_{j=1}^{k-1} \frac{1+\sqrt{1-\big(\gamma_j^{ni}\big)^2}}{2} \mathrm{Tr}\big[\sigma_z \otimes \sigma_z \rho_{A^{(n-1)s}A^{ni}}^{(1)}\big] \\ &= \sqrt{2}\gamma_k^{ni} \prod_{j=1}^{k-1} \frac{1+\sqrt{1-\big(\gamma_j^{ni}\big)^2}}{2}. \end{aligned} \tag{A7}$$

Substituting Eq. (A7) into Eq. (A4), we obtain

$$I_{0,\ldots,0}^{(k,\ldots,k)} = \frac{1}{(\sqrt{2})^{2^{n-1}}} \prod_{i=1}^{2^{n-1}} \left(\gamma_k^{ni} \prod_{j=1}^{k-1} \frac{1+\sqrt{1-\big(\gamma_j^{ni}\big)^2}}{2} \right). \tag{A8}$$

Similarly, we get

$$I_{1,\ldots,1}^{(k,\ldots,k)} = \frac{1}{(\sqrt{2})^{2^{n-1}}} \prod_{i=1}^{2^{n-1}} \left(\gamma_k^{ni} \prod_{j=1}^{k-1} \frac{1+\sqrt{1-\big(\gamma_j^{ni}\big)^2}}{2} \right). \tag{A9}$$

Substituting Eq. (A8) and Eq. (A9) into Eq. (A1), the expected $S_{(2^n-2)-\mathrm{local}}^{(k,\ldots,k)}$ value is given by

$$S_{(2^n-2)-\mathrm{local}}^{(k,\ldots,k)} = \sqrt{2}\; \sqrt[2^{n-1}]{\prod_{i=1}^{2^{n-1}} \left(\gamma_k^{ni} \prod_{j=1}^{k-1} \frac{1+\sqrt{1-\big(\gamma_j^{ni}\big)^2}}{2} \right)}. \tag{A10}$$

[1] J. S. Bell, Phys. Phys. Fiz. **1**, 195 (1964).
[2] D. Collins, N. Gisin, S. Popescu, D. Roberts, and V. Scarani, Phys. Rev. Lett. **88**, 170405 (2002).
[3] J. F. Clauser, M. A. Horne, A. Shimony, and R. A. Holt, Phys. Rev. Lett. **24**, 549 (1970).
[4] W. Tittel, J. Brendel, H. Zbinden, and N. Gisin, Phys. Rev. Lett. **81**, 3563 (1998).
[5] B. Hensen, H. Bernien, A. E. Dréau, A. Reiserer, N. Kalb, M. S. Blok, J. Ruitenberg, R. F. Vermeulen, R. N. Schouten, C. Abellán *et al.*, Nature (London) **526**, 682 (2015).
[6] R. Colbeck and A. Kent, J. Phys. A: Math. Theor. **44**, 095305 (2011).
[7] S. Pironio, A. Acín, S. Massar, A. B. de La Giroday, D. N. Matsukevich, P. Maunz, S. Olmschenk, D. Hayes, L. Luo, T. A. Manning *et al.*, Nature (London) **464**, 1021 (2010).
[8] A. Acín, N. Brunner, N. Gisin, S. Massar, S. Pironio, and V. Scarani, Phys. Rev. Lett. **98**, 230501 (2007).
[9] C. Branciard, N. Gisin, and S. Pironio, Phys. Rev. Lett. **104**, 170401 (2010).
[10] C. Branciard, D. Rosset, N. Gisin, and S. Pironio, Phys. Rev. A **85**, 032119 (2012).
[11] K. Mukherjee, B. Paul, and D. Sarkar, Quant. Inf. Process. **14**, 2025 (2015).
[12] A. Tavakoli, P. Skrzypczyk, D. Cavalcanti, and A. Acín, Phys. Rev. A **90**, 062109 (2014).
[13] A. Tavakoli, M. O. Renou, N. Gisin, and N. Brunner, New J. Phys. **19**, 073003 (2017).
[14] S. Munshi, R. Kumar, and A. K. Pan, Phys. Rev. A **104**, 042217 (2021).
[15] S. Munshi and A. K. Pan, Phys. Rev. A **105**, 032216 (2022).
[16] L. Yang, X. Qi, and J. Hou, Phys. Rev. A **104**, 042405 (2021).
[17] L. Yang, X. Qi, and J. Hou, Entropy **24**, 691 (2022).
[18] M.-O. Renou, E. Bäumer, S. Boreiri, N. Brunner, N. Gisin, and S. Beigi, Phys. Rev. Lett. **123**, 140401 (2019).
[19] P. Contreras-Tejada, C. Palazuelos, and J. I. de Vicente, Phys. Rev. Lett. **126**, 040501 (2021).
[20] M.-X. Luo, Phys. Rev. Res. **4**, 013203 (2022).
[21] J.-D. Bancal, N. Sangouard, and P. Sekatski, Phys. Rev. Lett. **121**, 250506 (2018).
[22] T. Morimae and K. Fujii, Phys. Rev. Lett. **111**, 020502 (2013).
[23] R. Silva, N. Gisin, Y. Guryanova, and S. Popescu, Phys. Rev. Lett. **114**, 250401 (2015).
[24] P. J. Brown and R. Colbeck, Phys. Rev. Lett. **125**, 090401 (2020).
[25] S. Mal, A. S. Majumdar, and D. Home, Mathematics **4**, 48 (2016).
[26] T. Zhang and S.-M. Fei, Phys. Rev. A **103**, 032216 (2021).
[27] T. Zhang, Q. Luo, and X. Huang, Quant. Inf. Process. **21**, 350 (2022).
[28] S. Saha, D. Das, S. Sasmal, D. Sarkar, K. Mukherjee, A. Roy, and S. S. Bhattacharya, Quant. Inf. Process. **18**, 42 (2019).
[29] C. Ren, X. Liu, W. Hou, T. Feng, and X. Zhou, Phys. Rev. A **105**, 052221 (2022).
[30] W. Hou, X. Liu, and C. Ren, Phys. Rev. A **105**, 042436 (2022).
[31] J.-H. Wang, Y.-J. Wang, L.-J. Wang, and Q. Chen, Phys. Rev. A **106**, 052412 (2022).
[32] S. S. Mahato and A. K. Pan, Phys. Rev. A **106**, 042218 (2022).
[33] T. Zhang, N. Jing, and S.-M. Fei, Front. Phys. **18**, 31302 (2023).
[34] Y.-L. Mao, Z.-D. Li, A. Steffinlongo, B. Guo, B. Liu, S. Xu, N. Gisin, A. Tavakoli, and J. Fan, Phys. Rev. Res. **5**, 013104 (2023).
[35] J. Haegeman, C. Lubich, I. Oseledets, B. Vandereycken, and F. Verstraete, Phys. Rev. B **94**, 165116 (2016).
[36] D. Suess, A. Eisfeld, and W. T. Strunz, Phys. Rev. Lett. **113**, 150403 (2014).
[37] M.-J. Hu, Z.-Y. Zhou, X.-M. Hu, C.-F. Li, G.-C. Guo, and Y.-S. Zhang, npj Quantum Inf. **4**, 63 (2018).